A NOVEL HUMAN-IN-THE-LOOP TESTING FACILITY FOR SPACE APPLICATIONS

M. Neves[1], *A. Seefried*[1], *M. Hagenfeldt*[2], *E. Sorbellini*[3], *L. Ferracina*[4], *R.Vittori*[4], *T. Bellmann*[1]

[1] German Aerospace Center (DLR)
[2] GMV Aerospace and Defence SAU (GMV)
[3] Thales Alenia Space (TAS)
[4] European Space Research and Technology Centre (ESTEC)

ABSTRACT

To analyse the interaction between the piloting astronaut and lunar lander dynamics while landing on the south pole of the moon, The European Space Agency (ESA) has initiated together with Thales Alenia Space (TAS), GMV Aerospace and Defence SAU (GMV) and The German Aerospace Centre (DLR) a project entitled *"Human-In-the-Loop Flight Vehicle Engineering"*. For this purpose, the DLR Robotic Motion Simulator (RMS) was transformed into a novel Human-in-the-Loop testing facility for space applications. The RMS represents a new class of motion simulators being currently developed at DLR that allow for extreme tilt angles and manoeuvres. It is based on an industrial 6 Degrees of Freedom (DOF) robot arm that is mounted onto a 10m long linear axis. The system therefore has a redundant 7 DOF architecture to induce motion cues onto an attached simulator cell. A highly modular simulator cell was configured for landing on the moon with three touch screens that were used to interact with the Human Machine Interface (HMI), Throttle and Joystick instruments, a virtual window to the outside, a headset and a surveillance camera for the piloting astronaut. The joystick features 3 DOFs and the throttle features adjustable damping along with many buttons that were used as inputs to the simulation. For the Moon landing scenery, a high-resolution lunar crater visualization based on DLR's Visualization 2 library was developed. Rocks and Boulders were distributed over the surface of the simulated region of the moon according to the Size-Frequency Distribution (SFD) for moon craters. ESA astronaut and test pilot Roberto Vittori tested various lunar landing manoeuvres using flight controls algorithms developed in HITL and motion simulation, provided by GMV, and was able to experience how the spacecraft behaves in critical phases of the lunar landing and intervene to control it. In one scenario the Landing GNC Automatic Mode was set to a landing zone where there were boulders. Vittori then had the option to intervene within a certain time window and, using touchscreens, select an alternative landing site. If needed, he was able to switch to Astronaut Manual Mode and pilot the lunar lander manually as it descended onto the lunar floor. Two Manual Control strategies were tested: Full Force / Torque Control and Rate Control. Two Motion cueing algorithms for low gravity environments were tested. Further experiments are planned.

Index Terms— Motion Simulation, Motion Cueing, Low Gravity Simulation, Lunar Landing

1. INTRODUCTION

Mankind first set step on the Moon on July, 1969 with the Apollo 11 National Aeronautics and Space Administration (NASA) Mission [1] starting thus a new era of crewed exploration of the Moon. Apollo 17, having left the Moon on December 14, 1972, marks the end of this era only four years later [2] [3].
Efforts from the International Space Exploration Coordination Group (ISECG) plan to refocus the human based exploration of the Moon, more than five decades after man last stepped on it [4].

The Lunar Orbital Platform-Gateway (LOP-G) is a space station that will be initially placed in a Near-Rectilinear Halo Orbit around the Moon allowing astronauts to depart from the LOP-G to land on the south pole of the moon [5].

To analyse the interaction between the piloting astronaut and lunar lander dynamics while landing on the south pole of the moon the European Space Agency (ESA) has initiated together with Thales Alenia Space (TAS), GMV Aerospace and Defence SAU (GMV) and the German Aerospace Center (DLR) a project entitled *Human-In-the-Loop Flight Vehicle Engineering*. This technology activity is lead in ESA by Dr. Luca Ferracina and it aims at establishing a preliminary design and the preliminary requirements for human landing involving Astronauts-in-the-Loop to improve robustness and reliability of the flight systems [5].

Moving-Base simulators have been an elemental tool for the development and testing of lunar landers. During the Apollo Era, a gantry based motion platform named the Lunar Landing Research Facility (LLRF) with a Lunar Excursion Module Simulator (LEMS) attached was used [6]. Shortly after, NASAs Vertical Motion Simulator (VMS) became operational and is still being used today [7]. In more recent

studies DLR's Robotic Motion Simulator (RMS) has shown its potential as a Lunar Landing (LL) simulator [3].

As final demonstration of the applicability of the developed Guidance, Navigation and Control (GNC) and Human Machine Interface (HMI) systems, a demonstration of the HITL scenario has been performed on the DLR RMS, in order to observe the interaction between the piloting astronaut and the lander system.

2. SETUP

2.1. DLR Robotic Motion Simulator

For this purpose, the DLR RMS was refitted into a novel Human-In-The-Loop (HITL) testing facility for space applications. The RMS represents a new class of motion simulators being currently developed at DLR that allow for extreme tilt angles and manoeuvres [8–13]. It is based on an industrial 6 Degrees of Freedom (DOF) robot arm that is mounted onto a 10m long linear axis forming a redundant 7 DOF architecture to induce motion cues onto an attached simulator cell. as illustrated in Fig. 1.
The RMS is fitted with two slip rings, one onto the q_1 axis and another onto the q_6 axis, that enable the simulator cell to endlessly rotate on its roll and yaw axis, when simulating lunar lander dynamics.

The distinctive advantages of the RMS over the traditional Steward-platform based simulators are a large rotational and translational workspace, that make the RMS one of the most dexterous serial kinematic simulators available, and a highly flexible system concerning different modular cockpit components and input devices.
On the other hand the RMS offers lower payload and accelerations when compared to its Steward-platform based counterparts [11]. The RMS is limited to a payload of 500 kg.

2.2. Simulator Cell

The RMS is fitted with a highly modular simulator cell that can be configured to best serve the simulation purpose intended, as illustrated in Fig. 2. The simulator cell features sitting modules with instrument bays and different instrument modules that are attachable to the sitting module. The simulator cell is fitted with a stereo-projection system and a multitude of safety devices. In its latest form, the RMS is used in combination with Virtual Reality (VR) glasses that track the pilots head position to deliver an immersive VR experience.

For the presented HITL scenario the seating module was configured as visible in Fig. 3. It features three touch-screens that were used to interact with the HMI software, non actuated Throttle and Joystick instruments, a virtual window to the outside, as well as a headset and a surveillance camera for the piloting astronaut. The VR glasses were removed for this experiment and the stereo-projection system was not used. The

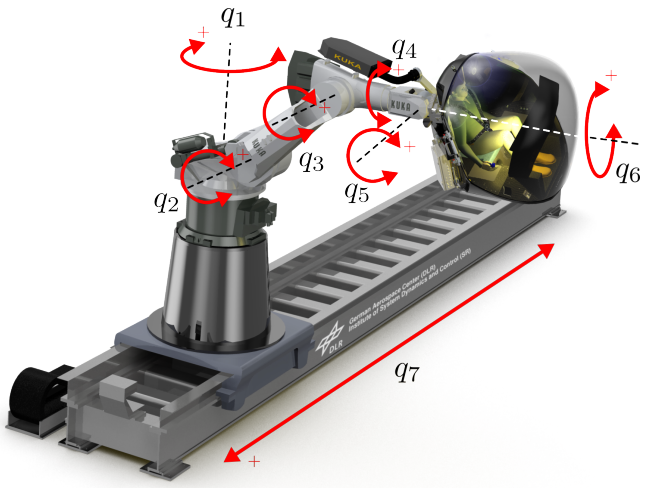

Fig. 1. DLR Robotic Motion Simulator (RMS) Overview, Showing Joint Locations and Turning Directions of the Robotic Platform

Fig. 2. Exploded View of DLR RMS's Simulator Cell Showing It's Modular Design

Fig. 3. Configured Seating Module for the Lunar Landing Experiment

piloting astronaut had to rely on the HMI, the LLs virtual window to the outside and the motion cues from the RMS in order to land safely.

2.3. Instruments

Commercially available Off-The-Shelf (COTS) components were chosen for this experiment. The joystick features 3 DOFs and the throttle allows for adjustable damping along with buttons that were used as inputs to the simulation. Using the buttons on the stick it was possible for the astronaut to fine tune the thrust from a certain sink rate on. By pressing a button, the current gravity acceleration of the lunar lander can be compensated by the thrust automatically (hold flag).

2.4. HMI

Project partner TAS provided user interfaces for manoeuvre control, including touch screen software. The HMI features a Primary Flight Display (PFD), a Navigation Display (ND) and a Multi-function Flight Display (MFD). The PFD provides the pilot with a Navball and avionic indicators. The ND features a choice between two outward facing GNC Cameras, Landing Site Retargeting options, flight data and a reachability map projected onto of the GNC Camera stream that give the piloting astronaut the ability to choose an obstacle free landing site. The MFD features four downward GNC Cameras and the status of the system.

2.5. Flight Assisted Controls and Dynamic Model of the Lunar Lander system

The flight assisted controls of the simulated lunar module were developed by GMV and adapted for the DLR simulator. The dynamic model of the lunar lander features its dynamics and kinematics, vehicle mass centring and inertia, sensors performance models and propulsion including fuel consumption of the lunar lander (and estimated remaining flight time) during the descent to be shown to the pilot on the HMI. The dynamic model outputs the flight state vectors (position, acceleration, angular velocity, orientation) necessary for the movement calculations of the Motion Simulator.
The controls in manual mode map the inputs of the stick and lever to the desired vehicle rates or torques (rate control or torque control) and thrust, respectively.
The flight assisted controls allows the lander to perform semi-autonomous, manual or hybrid manual landing during the demonstration. In the (semi)-autonomous mode, the astronaut can either let the lander land autonomously or use one of two retargeting windows during landing to choose a new landing site. In extreme contingency cases, the pilot can go into a hybrid manual or full manual mode and control the lander. Details concerning the flight assisted controls and dynamic model can be found in [14].

2.6. Moon Visualization

For the Moon landing scenery, a high-resolution lunar crater visualization based on DLR's Visualization 2 library [15] has been developed. This environment visualization is displayed on the virtual window inside the capsule (see Fig. 3), allowing the piloting astronaut to further asses the situation and the landers attitude. Furthermore, the visualization is also used for the observers of the experiment, showing the lander from an outside perspective to allow for an intuitive assessment of the flight state (See Fig. 4).

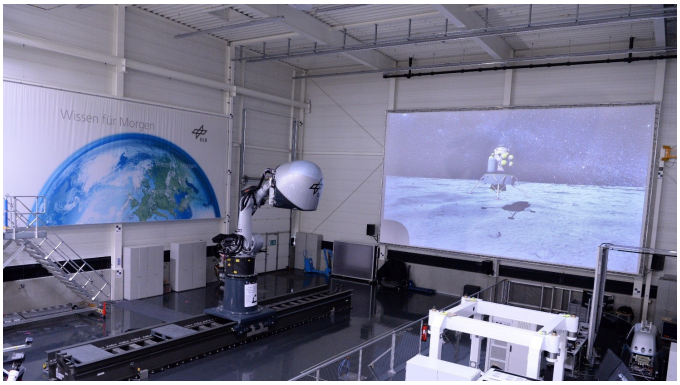

Fig. 4. The DLR Robotic Motion Simulator with the astronaut in the cell shortly before a landing. The maneuvers of the lunar lander can be observed on the large screen behind the simulator system

2.7. Environment

In order to achieve a realistic landing scenario environment, rocks are scattered on the lunar surface that must be taken into account when landing. The sizes and the distribution of the rocks have been generated according to [16] with parameters from [17]. The distribution of the sizes is shown in Fig. 5 and over the complete map there are about 1.7 million rocks.

For a safe landing, the lunar lander should not land on a rock so a *ground truth* is generated with help of the terrain and the information of the rocks. Following algorithm is used to evaluate, whether a point is safe to land on or not.

1. Set every point on the map to 'safe'
2. For every rock:
   (a) Define a circle with the radius of the rock plus the radius of the lunar lander
   (b) Set all points within that circle of the rock's position to 'unsafe'
3. For every 'safe' point:
   (a) Find the highest and lowest point within a radius of the lunar lander around the point

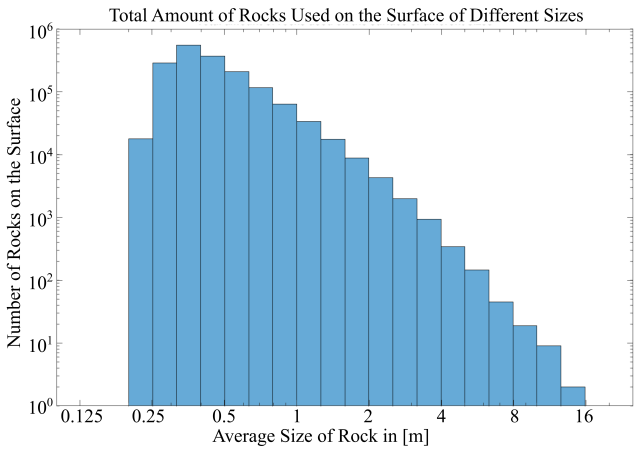

Fig. 5. Distribution of the different sizes of the rocks used in the simulation

(b) Calculate the slope between these two points

(c) If the slope exceeds a limit, the point is marked as 'unsafe'

All points that are marked as 'safe' are far enough away from a rock and the slope is below a given limit. This map is used to test whether the lander has landed on a safe spot at the moment of contact. An excerpt of the complete map is shown in Fig. 6

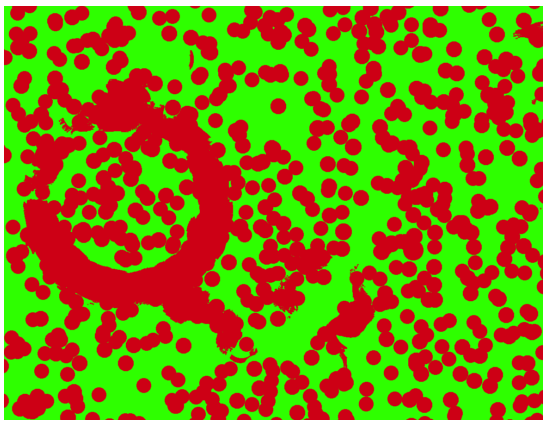

Fig. 6. Excerpt of safe map to determine where are safe spots to land. All green pixels are safe landing zones, far enough away from rocks and level enough for landing.

3. METHODS

3.1. Motion Cueing for Low-G Environments

The main problem with motion simulation on earth is, that it can barely provide an approximation of the descending landers space-craft dynamics. For terrestrial motion simulations,

Fig. 7. Visualization of the lunar surface with DLR SimVis [15].

the gravity vector is used as a measure to simulate long lasting accelerations via tilting of the simulator cell (also called tilt coordination [18]). For lunar landing applications, several factors have to be taken into account:

1. Moon has no atmosphere, and thus no air resistance, so the lander is either in free-fall or accelerates in the direction of its combined thrust vector.

2. Earths gravitational force of 1 g acting on the simulator is constant and only its direction can be changed from the point of view of the simulator pilot. So, in the simulator, the gravity vector can neither be varied, nor weightlessness can be simulated, a motion cueing algorithm on earth is bound to be imperfect.

Table 1. Tested Motion Cueing approaches for Low Gravity Scenarios on Earth

	1:1 Orientation Mapping	Classical Washout Filter
Rotational Vel.	correct	washed out
Translational Acc.	washed out	washed out
Simulated Thrust Force	wrong direction wrong magnitude	correct direction wrong magnitude

For this study, two different motion cueing algorithms have been tested and evaluated by the astronaut:

Motion Cueing A: 1:1 Orientation Mapping
Exact orientation and angular velocities: Using the large rotational workspace of the simulator, the orientation of the

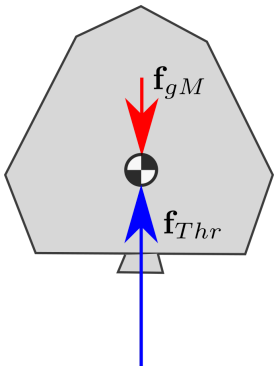

Fig. 8. A Lunar Lander With it's Main Booster Aligned with the Moon's Force of Gravity. The Booster Thrust Passes Through the Lander's Center of Mass

lunar lander has been recreated 1:1 in the simulator. In this case, false cues due to the wrong direction of the gravitational vector occur, but angular velocities of the lander are correct. Translational accelerations are added using a high-pass washout filter. The first column of Table 1 sums up this case.

Motion Cueing B: Classical Washout filter (from [10])
In this case, the tilt coordination is used to orient the capsule in a way, that the earths gravity points into the direction of the low-pass filtered acceleration of the lander. Angular velocities and translational accelerations of the lander are high-pass filtered, integrated and added to orientation and position of the capsule. In this case, the direction of the thrust force is correct, but its magnitude is wrong and angular velocities are only hinted. The second column of Table 1 sums up this case.

During the experiment, the astronaut tested both motion cueing algorithms in the same scenario.

3.2. Control approaches and landing site selection

The demonstrated experiment setup forsees the automatic landing of the lander on a predefined position with two opportunities to select another landing site (far range and close range landing site selection). During the far range landing site selection, a map showing unsafe landing areas is displayed and the astronaut has five seconds to select a new landing site and confirm the selection. This procedure is repeated with the close range landing site selection step, this time closer to the ground for final approach, as now new and better ground information is available concerning the landing site.

In contingency cases, where the automatic guidance system is not available, a manual control can be assumed by the piloting astronaut. Two manual control strategies were tested: force / torque control and rate control. In the torque control mode, the pilot commands torques around the lander principal axes and the attitude controller automatically generates the Reaction Control System (RCS) thruster control signals to perform the desired rotation. In rate control mode, the desired rate is given by the pilot and turing rates are generated accordingly.

3.3. Final approach and success evaluation

The simulation ends with the contact between lander and the ground. Several factors are evaluated and a report whether the landing was successful:

- Terrain Safety: Valid if the terrain respects requirements
- Vertical Speed (V_Z): Valid if below threshold.
- Horizontal Speed (V_X): Valid if below threshold.
- Lander Roll (Ψ_X): Valid if below threshold.
- Lander Pitch (Ψ_Y): Valid if below threshold.
- Angular Velocity relative to the X axis (Ω_X): Valid if below threshold.
- Angular Velocity relative to the Y axis (Ω_Y): Valid if below threshold.
- Angular Velocity relative to the Z axis (Ω_Z): Valid if below threshold.

After Landing the simulation results are displayed. Parameters will be shown in either Green or Red, indicating respectively if a parameter is respected or not.

A detailed terramechanic contact with the lunar soild, as in [19], is not calculated as it was out of the scope of this project.

4. EXPERIMENTAL RESULTS AND ANALYSIS

4.1. Experiments

ESA astronaut and test pilot Roberto Vittori tested various lunar landing manoeuvres using the flight controls algorithms provided by GMV, and was able to experience how the spacecraft behaves in critical phases of the lunar landing and intervene to control it. The experiments have been grouped in different scenarios: (semi-)autonomous mode with landing site selection, hybrid manual mode (rate control) and fully manual mode (torque control). After every experiment block, the astronaut has been debriefed and his experiences documented.
The following automated scenarios were simulated and tested:

1. Autonomous flight with no Landing Site (LS) selection
2. Semi-autonomous flight with LS selection at far range

3. Semi-autonomous flight with LS selection at close range

4. Semi-autonomous flight with LS selection at far and close range

The following manual flight scenarios were simulated and tested:

1. Manual mode flight engaged since terminal descent phase (TERM) with hold flag off

2. Manual mode flight engaged since TERM with hold flag on

3. Manual mode flight engaged since approach phase with hold flag off

4. Manual mode flight engaged since approach phase with hold flag on

The following rate controlled flight scenarios were simulated and tested:

1. Rate control manual mode flight engaged since TERM with hold flag off

2. Rate control manual mode flight engaged since TERM with hold flag on

3. Rate control manual mode flight engaged since approach phase with hold flag off

4. Rate control manual mode flight engaged since approach phase with hold flag on

In one scenario the Landing GNC Automatic Mode was set to a landing zone where there were boulders. The piloting astronaut then had the option to intervene within a certain time window and, using touchscreens, select an alternative landing site. If needed he was able to switch to Astronaut Manual Mode and pilot the lunar lander manually as it descended onto the lunar ground.

4.2. Results

4.2.1. Control of the lander

(Semi-)autonomous modes worked very well both with and without landing site selection. Full manual mode (torque control) has proven to be difficult to control, as with reduced support from the controller the workload for the pilot increases significantly and the control authorities for the modelled lander do not allow for piloting errors. The hybrid manual mode (rate control) has been perceived as more precise compared to torque control.

4.2.2. Controls

The combination of stick and throttle worked well in the dynamic environment of the motion simulator during flight, however, the throttle was deemed too unprecise for manual control during the final approach phase by the piloting astronaut. A larger movement range for the thrust lever has been suggested for better precision.

4.2.3. Low-G motion cueing

As expected, the Motion Cueing A (exact orientation and angular velocities) introduced large wrong specific forces due to the influence of the gravity acting on the simulator. During the early approach when the lander is tilted at an pitch angle of $\Psi_Y = -80°$ relative to the ground (see Fig. 9), the 1:1 display of the lander orientation by the simulator leads to a feeling of a strong lateral force caused by the gravity acting on the simulator. While the piloting astronaut was able to perform the task of landing the simulator, this wrong motion cue has been criticized as distracting.
The Motion Cueing B (Classical Washout Filter) was tested both in automatic and manual mode, and has been perceived by Roberto Vittori as the better representation of motion cues for a of a spacecraft in a reduced gravity environment. In this case, the simulator cockpit is upright most of the time, independent of the orientation of the simulated lander, as the only source of acceleration comes from the main thrusters firing downwards from the pilot. Only for the display of the washed-out angular velocities, the simulator cockpit is tilted. However, while the accelerations acting on the cockpit are displayed more precise, the perception of angular velocities has been perceived as considerable less compared with the Motion Cueing A, due to the use of filtered angular velocities. Imperfect in both cases was the non-changeable perception of lander deceleration, as the gravity vector cannot be varied in magnitude.

5. CONCLUSION AND FUTURE WORK

The overall experience of the astronaut has been described as very immersive and positive. The following feedback was received from the testing astronaut: The simulation is more intuitive/ realistic through motion simulation compared to a pure fixed based landing simulation. A further session addressing some of the mentioned issues has been agreed on. With ESA astronaut and test pilot Roberto Vittori successfully piloting the DLR prototype to land on the Moon, the team has achieved an important (technical) milestone of the HITL project.

For the next experiment, different improvements of the system are planned.

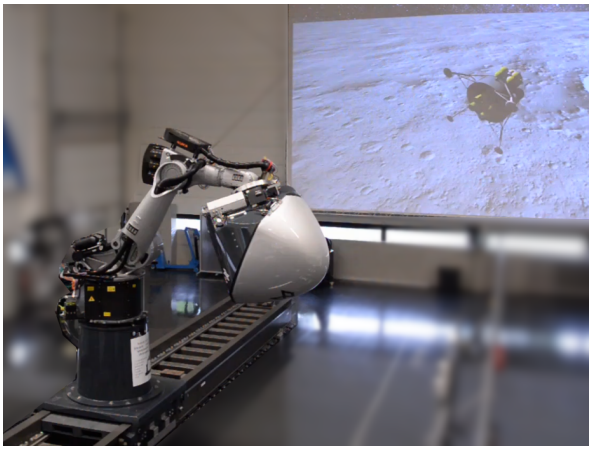

Fig. 9. The DLR Robotic Motion Simulator at the HITL start orientation when using Motion Cueing A

- In order to improve thrust control precision for the piloting astronaut the following approaches are considered:
  - A software based envelop adaption to change input range of throttle instrument according to landing stage will be introduced
  - A different throttle instrument with larger input range of motion (bigger actuation distance) will be implemented.
- Furthermore, fine-tuning of the washout filter parameters is planned to improve the perception of rotational motion cues.
- Another focus of the next tests will be improvements of simulation procedures, e.g. better check-lists and communication separation.

In potential follow up projects, emphasis will be put on the further development of other components, e.g. GNC and HMI systems to further improve flexibility, safety and handling during the landing manoeuvrer.

Acknowledgment

The project *"Human-in-the-Loop Flight Vehicle Engineering for Exploration Missions"* was funded by ESA.

6. REFERENCES

[1] United States. National Aeronautics and Space Administration, *Apollo 11 Mission Report*, Press kit. NASA, 1969.

[2] United States. National Aeronautics and Space Administration, *Apollo 17 Mission Report*, Press kit. NASA, 1973.

[3] Miguel Neves, "Human-In-The-Loop Controlled Lunar Landing Simulator ," M.S. thesis, Technical University of Munich, June 2019.

[4] The International Space Exploration Coordination Group (ISECG), "The International Space Exploration Coordination Group (ISECG)," https://www.globalspaceexploration.org/, 2022, [Online; accessed 01-May-2022].

[5] ESA, "ESA Astronaut Performs Simulated Polar Moon Landing," https://www.esa.int/Enabling_Support/Space_Engineering_Technology/ESA_astronaut_performs_simulated_polar_Moon_landing, 2022, [Online; accessed 02-May-2022].

[6] Nasa Langley Research Center, "Landing and Impact Research Facility (LANDIR)," https://researchdirectorate.larc.nasa.gov/files/2015/08/landir_factsheet.pdf, 2019, [Online; accessed 15-May-2019].

[7] Bimal L Aponso, Steven D Beard, and Jeffery A Schroeder, "The Nasa Ames Vertical Motion Simulator–a Facility Engineered for Realism," in *Proceedings of the royal aeronautical society spring flight simulation conference*. Citeseer, 2009, p. 4.

[8] Tobias Bellmann, Johann Heindl, Matthias Hellerer, Richard Kuchar, Karan Sharma, and Gerd Hirzinger, "The DLR Robot Motion Simulator Part I: Design and Setup," in *2011 IEEE International Conference on Robotics and Automation*. IEEE, 2011, pp. 4694–4701.

[9] Tobias Bellmann, Martin Otter, and Gerd Hirzinger, "The DLR Robot Motion Simulator Part II : Optimization Based Path-planning," in *IEEE International Conference on Robotics and Automation*, 2011.

[10] Tobias Bellmann, *Optimierungsbasierte Bahnplanung für Interaktive Robotische Bewegungssimulatoren*, Ph.D. thesis, Universität der Bundeswehr München, 2014.

[11] Tobias Bellmann and Andreas Labusch, "Next Generation Pilot Training with Robot-based Flight Simulators," in *Flight Simulation Conference 2014: The Future of Flight Training Devices*, Royal Aeronautical Society, Ed., 2015.

[12] Thomas Lombaerts, Gertjan Looye, Andreas Seefried, Miguel Neves, and Tobias Bellmann, "Development

and Concept Demonstration of a Physics Based Adaptive Flight Envelope Protection Algorithm," *IFAC-PapersOnLine*, vol. 49, no. 5, pp. 248–253, 2016.

[13] Andreas Seefried, Alexander Pollok, Richard Kuchar, Matthias Hellerer, Martin Leitner, Daniel Milz, Christian Schallert, Thiemo Kier, Gertjan Looye, and Tobias Bellmann, "Multi-domain Flight Simulation with the DLR Robotic Motion Simulator," in *Spring Simulation Conference 2019*, 05 2019.

[14] Miguel Hagenfeldt, Briz Jose Francisco, Vincenzo Pesce, Euginio Sorbellini, Mario Pessana, Tobias Bellmann, Luca Ferracina, and Roberto Vittori, "Human In-the-loop Flight Controls Assessment for Moon Descent and Landing Vehicles," in *Proceedings of the 2nd international Conference on Flight Vehicles, Aerothermodynamics and Re-entry Missions and Engineering (FAR)*, 2022.

[15] Sebastian Kümper, Matthias Hellerer, and Tobias Bellmann, "DLR Visualization 2 Library - Real-Time Graphical Environments for Virtual Commissioning," in *14th Modelica Conference*, Martin Sjölund, Lena Buffoni, Adrian Pop, and Lennart Ochel, Eds. September 2021, pp. 197–204, Modelica Association and Linköping University Electronic Press.

[16] Fabian Buse, Antoine Pignede, Jean Bertrand, Sébastien Goulte, and Sandra Lagebarre, "MMX Rover Simulation - Robotic Simulations for Phobos Operations," in *Proceedings of the 2022 IEEE Aerospace Conference, 5-12 March 2022, Big Sky, MT, USA*, Piscataway, NJ, USA, 2022, IEEE Aerospace Conference.

[17] WR Muehlberger, RM Batson, EL Boudette, CM Duke, RE Eggleton, DP Elston, AW England, VL Freeman, MH Hait, TA Hall, et al., "Preliminary Geologic Investigation of the Apollo 16 Landing Site," 1972.

[18] Peter R Grant and Lloyd D Reid, "Motion Washout Filter Tuning: Rules and Requirements," *Journal of Aircraft*, vol. 34, no. 2, pp. 145–151, 1997.

[19] Fabian Buse, "Using Superposition of Local Soil Flow Fields to Improve Soil Deformation in the DLR Soil Contact Model-SCM," in *5th Joint International Conference on Multibody System Dynamics*, Oktober 2018.